

# Linear and Nonlinear Schrödinger Equations on Simple Networks

Radu C. Cascaval and C. Travis Hunter

**Abstract.** Recent theoretical developments in the study of initial-boundary value problems for linear and nonlinear equations have motivated further studies of interface problems for PDEs posed on networks. We investigate the scattering (transmission and reflection) of pulses at interfaces and at bifurcations for the nonlinear Schrödinger (NLS) equation, as a prototype model for bidirectional wave propagation in physical media. NLS equation belongs to an entire class of nonlinear models, called integrable models, for which an intimate relationship exists between their solutions and the compatibility of a linear system (known as the scattering problem). Numerical simulations of such models posed on networks indicate that, even when the underlying equations are genuinely nonlinear, scattering at junctions still occurs in a linear fashion. This is consistent with similar behavior observed in other nonlinear systems.

## 1 Introduction

Wave propagation phenomena on networks have received much attention in the applied mathematics community lately. Among the notable areas of application are modeling the pressure waves in the circulatory system ([1], [5], [10]), action potential in neurons ([15]), and problems in traffic flow ([14]). One common focus of research in these application areas is understanding the evolution of pulses along the network, in particular the reflection and transmission of pulses at the junctions and their collective effect on the dynamics of an incoming pulse.

In this study, the nonlinear Schrödinger (NLS) equation (see below) is chosen as a prototype of the underlying evolution equation, posed on simple networks. Our choice was made based on the fact that NLS admits localized pulses traveling in both directions, hence it can support both transmitted and reflected pulses in the network. It is also among the most studied among of the integrable systems. Note that in physical applications, such as in optical communications, NLS often appears as a model for unidirectional evolution, with role of the variables 'time'  $t$  and 'space'  $x$  interchanged. When posed on the real line, the (focusing) nonlinear Schrödinger (NLS) equation

$$iq_t + q_{xx} + 2|q|^2q = 0, \quad x \in (-\infty, \infty), \quad t \geq 0, \quad (1)$$

admits a family of special solutions, the one-solitons, which are of the form  $q_{a,c,x_0}(x, t) =$

$a \operatorname{sech}[a(x - x_0 - ct)]e^{i[\frac{1}{2}cx + (a^2 - \frac{1}{4}c^2)t]}$  where  $a > 0$  is the peak amplitude,  $c \in \mathbb{R}$  is the speed of the envelope pulse,  $x_0$  is the position of the center of mass at time  $t = 0$ . Other special solutions (the  $N$ -solitons) can be obtained (e.g. via dressing methods) using the Zakharov-Shabat operator

$$L\Psi = i \begin{pmatrix} \frac{d}{dx} & -q \\ -\bar{q} & -\frac{d}{dx} \end{pmatrix} \Psi, \quad \Psi = \Psi(x, k) = [\psi_1, \psi_2]^T. \quad (2)$$

In fact, (NLS) is the compatibility condition for the system of linear equations:

$$\begin{aligned} \Psi_x &= -ik[\sigma_3, \Psi] + Q(x, t)\Psi \\ \Psi_t &= -2ik^2[\sigma_3, \Psi] + \tilde{Q}(x, t; k)\Psi \end{aligned} \quad (3)$$

where  $\sigma_3 = \operatorname{diag}\{1, -1\}$ ,  $Q = \begin{pmatrix} 0 & q \\ -\bar{q} & 0 \end{pmatrix}$  and  $\tilde{Q}(k) = 2kQ - iQ_x\sigma_3 + i|q|^2\sigma_3$ ,  $k \in \mathbb{C}$ . The first linear equation is another way of writing the eigenvalue problem for the operator  $L$ :  $L\Psi = k\Psi$ , while the second describes the time evolution of the wave functions  $\Psi = \Psi(t, k)$ .

The initial-boundary value problem for NLS turns out to be much more complicated due to the loss of 'integrability' at the boundary. Recent developments in this direction have been able to overcome some of these difficulties and introduced new open problems [6], [13]. It turns out that a satisfactory inverse scattering framework can be effectively employed only for certain boundary conditions (so-called linearizable boundary conditions for the half line problem), such as homogeneous Dirichlet, Neumann or Robin conditions. In each of these situations, the interaction of pulses with the boundary behaves more or less as expected (complete or partial reflection, with a corresponding phase shift), and can be interpreted using extensions to the full line problem and the presence of 'ghost' pulses [4] in the exterior of the domain.

In this paper we study a new type of boundary condition for the half-line problem. Our primary objective is to understand how pulses interact with junctions in a network. It has been observed in other systems (such as Benjamin-Bona-Mahony equation [5]) that this interaction is (surprisingly) linear when the incoming and transmitted (reflected) speeds and amplitudes are compared. It is the author's belief that the NLS context is the most natural one in which to study this phenomenon and develop a theoretical underpinning to explain it. This study is the first one in this effort. The layout of the paper is as follows: in Section 2 we introduce the relevant theory for the initial-boundary value problem on the half-line for both linear and nonlinear Schrödinger equations. Section 3 presents the extension the simple networks, such as Y-junctions, including a discussion on the well-posedness of this problem. Section 4 details some preliminary numerical studies which illustrate the pulse scattering phenomenon.

## 2 Half-Line Problem

### 2.1 Linear Schrödinger equation on the half-line

Consider first the linear Schrödinger equation on the half-line:

$$iq_t + q_{xx} = 0, \quad x \in [0, \infty), \quad t > 0 \quad (4)$$

Given an initial data  $q(x, 0) = q_0(x), x \geq 0$ , with Fourier transform

$$\hat{q}_0(k) = \int_0^\infty e^{-ikx} q_0(x) dx, \quad \text{Im } k \leq 0$$

an integral representation formula for the solution of (4) is (see e.g. [12])

$$q(x, t) = \frac{1}{2\pi} \int_{-\infty}^\infty e^{ikx - ik^2 t} \hat{q}_0(k) dk - \frac{1}{2\pi} \int_{\partial D^+} e^{ikx - ik^2 t} \tilde{g}(k, t) dk \quad (5)$$

where

$$\tilde{g}(k, t) = \int_0^t e^{ik^2 \tau} [kg_0(\tau) - ig_1(\tau)] d\tau.$$

where  $\partial D^+$  is the boundary of the 1st quadrant in the complex plane parametrized such that the domain remains on the left side. Here we use the notation for the Dirichlet and Neumann boundary data at  $x = 0$ ,

$$q(0, t) = g_0(t), \quad q_x(0, t) = g_1(t)$$

respectively. Note that the integral representation depends on both the Dirichlet and Neumann boundary conditions. On the other hand, it is well-known that the initial-boundary value problem for (4) is well posed by assigning only one type of boundary data, e.g. Dirichlet:

$$\begin{aligned} iq_t + q_{xx} &= 0, \quad x \in [0, \infty), \quad t \in (0, T) \\ q(x, 0) &= q_0(x) \\ q(0, t) &= g_0(t) \quad (\text{Dirichlet boundary at } x = 0) \end{aligned}$$

in which case the other boundary condition becomes unknown in the representation formula (5).

The Dirichlet-to-Neumann map can be derived, in the half-line case, using the global relation of the Lax pair formulation of the linear Schrödinger equation (see [13] page 284). More specifically,

$$g_1(t) = q_x(0, t) = -e^{\frac{i\pi}{4}} \left[ \frac{1}{\sqrt{t}} \int_0^\infty e^{\frac{ix^2}{4t}} q_0'(x) dx + \frac{1}{\sqrt{\pi}} \int_0^t \frac{\dot{g}_0(\tau)}{\sqrt{t-\tau}} d\tau \right]. \quad (6)$$

The last term is the so-called fractional derivative of the boundary data  $g_0$ . Recall the definition of the Riemann-Liouville integral w.r.t  $t$  of (fractional) order  $\alpha > 0$ , [18],

$$I^\alpha f(t) = \frac{1}{\Gamma(\alpha)} \int_0^t f(\tau) (t-\tau)^{\alpha-1} d\tau$$

and its semigroup property

$$I^\alpha I^\beta f(t) = I^{\alpha+\beta} f(t), \quad \alpha, \beta > 0.$$

The fractional derivative (in the sense of Caputo) is defined as

$$\partial_t^{1/2} f(t) := I^{1/2} \partial_t f(t) = \frac{1}{\sqrt{\pi}} \int_0^t \frac{\partial_\tau f(\tau)}{\sqrt{t-\tau}} d\tau.$$

## 2.2 Nonlinear Schrödinger equation on the half-line

The NLS on the half line  $\mathbb{R}^+ = [0, +\infty)$  with prescribed Dirichlet boundary conditions

$$iq_t + q_{xx} + 2|q|^2q = 0, \quad x \in [0, \infty), \quad t \geq 0, \quad (7)$$

$$q(0, t) = g_0(t), \quad t \geq 0, \quad q(x, 0) = q_0(x), \quad x \geq 0 \quad (8)$$

is well-posed (see e.g. [8] )for sufficiently smooth and compatible initial and boundary conditions. A scattering and inverse scattering transform has been developed recently (see [13] and the reference herein.) It is formulated in terms of the Dirichlet data  $g_0(t) = q(0, t)$  and the Neumann data

$$g_1(t) := q_x(0, t),$$

the latter one not being prescribed in the problem, hence it needs to be treated as unknown data. Thus, the key problem is: given  $g_0(t)$  and  $q_0(x)$ , find an expression for  $g_1(t)$ . The inverse problem is then reduced to a Riemann-Hilbert problem. For sake of brevity, we include here only the details of constructing the Dirichlet-to-Neumann (DtN) map, referring the reader to [13] for the problem of recovering the potential  $q(x, t)$  from the spectral data.

**The case  $q_0 \equiv 0$ :** The following is a representation of the Dirichlet-to-Neumann map for the case  $q_0(x) \equiv 0$  (see [7] Proposition 1 and [20]):

$$\begin{aligned} g_1(t) &= g_0(t)M_2(t, t) - \frac{e^{-i\pi/4}}{\sqrt{\pi}} \int_0^t \frac{\partial_\tau M_1(t, 2\tau - t)}{\sqrt{t - \tau}} d\tau \\ &= g_0(t)M_2(t, t) - e^{-i\pi/4} \partial_\tau^{1/2} M_1(t, 2\tau - t)|_{\tau=t}. \end{aligned} \quad (9)$$

Here  $M_1 = M_1(t, s)$  and  $M_2 = M_2(t, s)$  (together with  $L_1 = L_1(t, s)$  and  $L_2 = L_2(t, s)$ ) are functions, defined on the domain  $\Lambda = \{(t, s) | t \geq 0, -t \leq s \leq t\}$ , which satisfy the following hyperbolic system

$$\begin{cases} L_{1t} - L_{1s} = ig_1(t)L_2 + \alpha(t)M_1 + \beta(t)M_2 \\ L_{2t} + L_{2s} = i\overline{g_1(t)}L_1 - \alpha(t)M_2 - \overline{\beta(t)}M_1 \\ M_{1t} - M_{1s} = 2g_0(t)L_2 + ig_1(t)M_2 \\ M_{2t} + M_{2s} = -2\overline{g_0(t)}L_1 - i\rho\overline{g_1(t)}M_1 \end{cases} \quad (10)$$

with the coefficients

$$\alpha(t) = -\frac{1}{2}(g_0\overline{g_1} - \overline{g_0}g_1), \quad \beta(t) = \frac{1}{2}(ig_0 + |g_0|^2g_0) \quad (11)$$

and 'initial' data

$$L_1(t, t) = \frac{i}{2}g_1(t), \quad M_1(t, t) = g_0(t), \quad L_2(t, -t) = M_2(t, -t) = 0 \quad (12)$$

Finally, the functions  $L_1, M_1, L_2, M_2$  are used in the Gelfand-Levitan-Marchenko representation of the wave function at the boundary  $x = 0$ :

$$\Phi(0, t, k) = \begin{pmatrix} 0 \\ e^{2ik^2t} \end{pmatrix} + \int_{-t}^t \begin{pmatrix} L_1 - \frac{i}{2}g_0(t)M_2(t, s) + kM_1(t, s) \\ L_2 - \frac{i}{2}g_0(t)M_1(t, s) + kM_2(t, s) \end{pmatrix} e^{2ik^2s} ds.$$

**The general case**  $q_0(x)$ : Remarkably, similar auxiliary functions  $L_i, M_i, i = 1, 2$  solving the same system appear in the DtN map in the general case  $q_0 \neq 0$  ([7] Proposition 3). Given an (nonzero) initial condition  $q_0(x)$  in the Schwartz class on  $\mathbb{R}_+$ , we define the spectral functions  $a(k)$  and  $b(k)$  for  $k \in \mathbb{C}^+$  (with  $\Im k \geq 0$ ) as follows:

$$a(k) = \psi_2(0, k), \quad b(k) = \psi_1(0, k),$$

where the vector  $\Psi = [\psi_1, \psi_2]^T$  is the unique solution of the system

$$\begin{aligned} \psi_{1,x} &= -ik\psi_1 + q_0(x)\psi_2 \\ \psi_{2,x} &= -\bar{q}_0(x)\psi_1 + ik\psi_2, \end{aligned}$$

satisfying  $\lim_{x \rightarrow \infty} e^{-ikx}\Psi = [0, 1]^T$  as  $x \rightarrow \infty$ . Denote

$$R(k) = \frac{b(k)}{a(k)} = \frac{\psi_1(0, k)}{\psi_2(0, k)}.$$

Then, the Dirichlet-to-Neumann map reads:

$$\begin{aligned} g_1(t) &= g_0(t)M_2(t, t) - \frac{e^{-i\pi/4}}{\sqrt{\pi}} \int_0^t \frac{\partial_\tau M_1(t, 2\tau - t)}{\sqrt{t - \tau}} d\tau + \frac{4i}{\pi} R_1(t) \\ &\quad + g_0(t) \frac{4}{\pi} \int_0^t R_1(\tau) \overline{M_1(t, 2\tau - t)} d\tau \\ &\quad + \frac{8i}{\pi} \int_0^t R_1(\tau) \overline{L_2(t, 2\tau - t)} + R_2(\tau) \overline{M_2(t, 2\tau - t)} d\tau. \end{aligned} \tag{13}$$

Here we used, for convenience, the notations

$$R_1(t) = \int_{\partial D^+} kR(k)e^{-4ik^2t} dk, \quad R_2(t) = \int_{\partial D^+} k^2R(k)e^{-4ik^2t} dk,$$

the integration being counterclockwise on the boundary  $\partial D^+ = (i\infty, 0] \cup [0, \infty)$  of  $D^+ = \{k \in \mathbb{C} \mid \Re k \geq 0, \Im k \geq 0\}$ , the first quadrant in the complex plan as before. This is in the case that  $a(k)$  has no poles in  $D^+$ . If  $a(k)$  has poles in  $D^+$ , then the contour of integration need to be chosen above all poles of  $a(k)$ .

As expected, the DtN map (13) trivially reduces to (9) in the case  $q_0(x) \equiv 0$ , since in that case  $R(k) \equiv 0$ .

### 3 Simple Network Problem

In this section we extend the considerations in the previous section to the case of a finite network, which is a collection of spatial edges  $e \in \mathcal{E}$  connected at the vertices  $v \in \mathcal{V}$ . We denote  $\mathcal{N} = \bigcup_{e \in \mathcal{E}} e$  the spatial domain of the network. The degree of a vertex, denoted  $\deg v$ , is the total number of edges which share  $v$  as an end-point. We need to specify junction conditions at vertices of degree  $\geq 2$  and boundary conditions at vertices of degree  $= 1$  (also known as terminal conditions). We parametrize each edge  $e_i$  of the network with

either  $[0, l_i]$ , if they have finite length  $l_i$ , or with a semi-axis  $[0, \infty)$ . This fixed but arbitrary parameterization implies that we must make a choice of orientation for each edge. Since the underlying equations we consider in this work don't involve the first derivative operator, but only the second derivative, the choice of the orientation can be made arbitrary. For simplicity we assume the same (linear or nonlinear Schrödinger) equation governs the evolution on each edge.

To be more specific, when the network is a simple Y-junction (see Figure 1) with one vertex and three infinite edges, as depicted in the figure below, each edge is parametrized so that it is identified with a semi-axis: parent edge is  $e_1 = (-\infty, 0]$  and the two daughter edges  $e_2 = e_3 = [0, +\infty)$ .

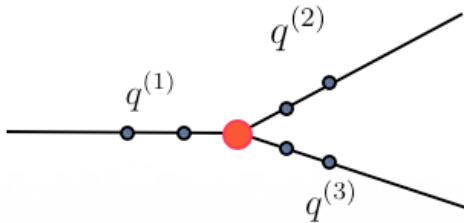


Figure 1: NLS potential on a Y-junction

For this simple 3-edge junction, we consider the 'standard' junction conditions at the vertex:

$$\begin{aligned} q^{(1)}(0, t) &= q^{(2)}(0, t) = q^{(3)}(0, t) \\ q_x^{(1)}(0, t) &= q_x^{(2)}(0, t) + q_x^{(3)}(0, t) \end{aligned}$$

To study the transmission and reflection of pulses originating in the parent edge, we assume that initial conditions on the daughter edges are the same. Hence we identify the daughter edges (two for the Y-junction) and assume the spatial domain is the entire real axis  $(-\infty, 0] \cup [0, \infty)$ . Denote  $q(x, t) = q^-(x, t)$  if  $x \leq 0$  and  $q(x, t) = q^+(x, t)$  if  $x \geq 0$ . At the interface we have continuity but a 'jump' in the left and right derivatives:

$$q^-(0, t) = q^+(0, t), \quad q_x^-(0, t) = \gamma q_x^+(0, t), \quad \gamma = \deg v - 1$$

We will refer to this simplified situation as the interface problem below. It is also worth mentioning that other junction conditions have been studied in [19], although they lead to trivial (upon rescaling) bifurcations of incoming pulses.

### 3.1 Interface problem for the linear Schrödinger equation

Here we consider again the linear Schrödinger (LS) equation as the underlying equation. More specifically,  $q$  satisfies the same equation (4) on both positive and negative semi-axis, is continuous at  $x = 0$  and has a jump in the derivative:

$$\begin{aligned} q^-(0, t) &= q^+(0, t) \\ q_x^-(0, t) &= \gamma q_x^+(0, t) \end{aligned}$$

The interface problem can also be viewed as a forced LS equation on the real line, where the (impulsive) forcing is occurring at the interface  $x = 0$ :

$$iq_t + q_{xx} = \beta\delta_0(x)q_x.$$

with  $\beta = \frac{2(\gamma-1)}{\gamma+1}$ . Applying formula (6) for both semi-axis, we obtain:

$$\begin{aligned} 0 &= q_x^-(0, t) - \gamma q_x^+(0, t) \\ &= -e^{\frac{i\pi}{4}} \left[ -\frac{1}{\sqrt{t}} \int_{-\infty}^0 e^{\frac{ix^2}{4t}} q_0'(x) dx + \frac{\gamma}{\sqrt{t}} \int_0^{\infty} e^{\frac{ix^2}{4t}} q_0'(x) dx + \frac{1+\gamma}{\sqrt{\pi}} \int_0^t \frac{\dot{g}_0(\tau)}{\sqrt{t-\tau}} d\tau \right]. \end{aligned}$$

so

$$\int_0^t \frac{\dot{g}_0(\tau)}{\sqrt{t-\tau}} d\tau = \sqrt{\frac{\pi}{t}} \left[ \frac{1}{\gamma+1} \int_{-\infty}^0 e^{\frac{ix^2}{4t}} q_0'(x) dx - \frac{\gamma}{\gamma+1} \int_0^{\infty} e^{\frac{ix^2}{4t}} q_0'(x) dx \right] \quad (14)$$

Using the fact that  $I_t^{1/2}$  is the left inverse of  $\partial_t^{1/2}$ , one can also compute from (14) the Dirichlet data

$$g_0(t) = q(0, t) = I_t^{1/2} \left[ \int_0^t \frac{\dot{g}_0(\tau)}{\sqrt{t-\tau}} d\tau \right]$$

From (6) and (14) we also derive the explicit representation for the Neumann data at the interface (say for the  $x > 0$  problem)

$$g_1(t) = q_x^+(0, t) = -\frac{e^{\frac{i\pi}{4}}}{\sqrt{t}} \frac{1}{\gamma+1} \int_{-\infty}^{\infty} e^{\frac{ix^2}{4t}} q_0'(x) dx. \quad (15)$$

Finally, one uses the representation (5) to obtain  $q^+(x, t), x > 0$  and, similarly,  $q^-(x, t), x < 0$ .

### 3.2 Interface problem for the nonlinear Schrödinger equation

The NLS equation with the standard junction and terminal conditions mentioned above is well-posed on a finite network, but we postpone this discussion until the next section. Here we present the analogous construction of the Dirichlet and Neumann data for the interface NLS. As expected, we will employ the complicated DtN map derived for the initial boundary value problem described in Sect 2.2. The goal of this section is to show how one can derive the Dirichlet data (and hence the Neumann data on both sides) at the interface.

Consider the interface condition for NLS potentials  $q^-$  and  $q^+$ :

$$\begin{cases} q^-(0, t) = q^+(0, t) & [= g_0(t)] \\ q_x^-(0, t) = \gamma q_x^+(0, t) & [= \gamma g_1(t)] \end{cases}$$

and the initial condition

$$q_0(x) = \begin{cases} q_0^-(x), & x < 0 \\ 0, & x \geq 0 \end{cases}$$

supported on the left half-line  $(-\infty, 0)$ , that is  $q_0^+(x) = 0$ , for all  $x \in [0, \infty)$ . For the numerical studies in the next section, we will take as initial condition a soliton that is sufficiently far away (to the left) and moving to the right, towards the interface.

For each of the half axis, we consider the auxiliary functions  $X^- = [L_1^-, L_2^-, M_1^-, M_2^-]^T$  and  $X^+ = [L_1^+, L_2^+, M_1^+, M_2^+]^T$ , which satisfy the following system of eight hyperbolic equations (written in the abbreviated form):

$$\begin{aligned} X_t^- - JX_s^- &= [-\gamma A(t) + B(t)]X^-, \\ X_t^+ - JX_s^+ &= [A(t) + B(t)]X^+ \end{aligned} \quad (16)$$

where we introduced the following  $4 \times 4$  block matrices:

$$J = \begin{pmatrix} \sigma_3 & 0 \\ 0 & \sigma_3 \end{pmatrix}, \quad A(t) = \begin{pmatrix} 0 & ig_1(t) & \alpha(t) & 0 \\ ig_1(t) & 0 & 0 & -\alpha(t) \\ 0 & 0 & 0 & ig_1(t) \\ 0 & 0 & ig_1(t) & 0 \end{pmatrix},$$

$$B(t) = \begin{pmatrix} 0 & 0 & 0 & \beta(t) \\ 0 & 0 & -\beta(t) & 0 \\ 0 & 2g_0(t) & 0 & 0 \\ -2\overline{g_0(t)} & 0 & 0 & 0 \end{pmatrix}$$

Note that this notation is convenient since  $B$  depends only on the Dirichlet data  $g_0(t)$ , while  $A$  depends in a linear fashion on the Neumann data  $g_1(t)$ . [Recall from (11) that  $\alpha(t) = -\frac{1}{2}(g_0\overline{g_1} - \overline{g_0}g_1)$ ,  $\beta(t) = \frac{1}{2}(ig_0 + |g_0|^2g_0)$ ]. The negative sign in (16)<sub>1</sub> in front of  $\gamma$  comes from the fact that the Neumann data on the left half-line  $(-\infty, 0]$  gets a minus sign upon change of variables  $x \rightarrow -x$ .

Combining (9) written for  $[0, \infty)$  and (13) for  $(-\infty, 0]$  we obtain the following representation for  $g_0(t)$ :

$$g_0(t) = \frac{e^{-i\pi/4}\partial^{1/2}(M_1^- - \gamma M_1^+)(t, t) + \frac{4i}{\pi}R_1(t) + \frac{8i}{\pi}(R_1 *_s \overline{L_2^-})(t) + (R_2 *_s \overline{M_2^-})(t)}{(M_2^- - \gamma M_2^+)(t, t) + \frac{4}{\pi}(R_1 *_s \overline{M_1^-})(t)} \quad (17)$$

Here, again, we used a simplified notation:

$$\partial^{1/2}f(t, t) = \partial_\tau^{1/2}f(t, 2\tau - t)|_{\tau=t} = \frac{1}{\sqrt{\pi}} \int_0^t \frac{\partial_\tau f(t, 2\tau - t)}{\sqrt{t - \tau}} d\tau$$

and the convolutions  $(R_i *_s f)(t) = \int_0^t R_i(\tau)f(t, 2\tau - t) d\tau$ , for  $i = 1, 2$ .

The right hand side of (17) is a function of  $t$  alone, assuming the system (16) has been solved up to time  $t$ . For a fixed  $t$ , it is computed using only the values of the auxiliary functions  $X^-$  and  $X^+$  on the line segment  $\Lambda_t = \{(t, s) \mid -t \leq s \leq t\}$ . Then the Neumann data is computed using (9):

$$g_1(t) = g_0(t)M_2^+(t, t) - \partial^{1/2}M_1^+(t, t). \quad (18)$$

Consequently, the system (16)–(18) can be solved (at least locally) in time starting with the initial conditions provided in (12). Global (in time) existence of solutions to this system remains an open problem (see also [13]). Numerical approximations of solutions to the system (16)–(18) are detailed in the last section.

### 3.3 Finite network problem for NLS

In this section we discuss the NLS equation posed on a finite network (with finite or infinite length edges).

$$iq_t + q_{xx} + 2|q|^2q = 0, \quad x \in \mathcal{N}, \quad t \geq 0 \quad (19)$$

where  $T = \bigcup_{e \in \mathcal{E}}$  is the spatial domain of a finite network.

For any finite length terminal edge, we impose homogeneous boundary conditions, e.g. Dirichlet or Neumann conditions. For infinite length terminal edges, we assume the solutions (and its derivatives) decay at the infinite end, e.g.  $q, q_x, q_{xx} \rightarrow 0$  as  $x \rightarrow \infty$ . Even the more restrictive Schwartz class at the infinite end suffices for our purposes here, since, for computational purposes, the infinite edges will be replaced by finite edges. Artificial boundary conditions (ABCs) based on the DtN map will be imposed at those artificial boundaries.

The following integrals (mass and energy) are conserved by the NLS equation when posed on the finite network  $\mathcal{N}$ :

$$I_0(t) = \int_{\mathcal{N}} |q|^2 dx, \quad I_1(t) = \int_{\mathcal{N}} |q_x|^2 - |q|^4 dx$$

The invariance easily follows from the identities

$$(|q|^2)_t = -2\Im(\bar{q}q_x)_x$$

$$(|q_x|^2 - |q|^4)_t = 2\Re(\bar{q}_t q_x)_x$$

which are satisfied by any NLS solution  $q = q(x, t)$ . Hence, for each edge  $e \in \mathcal{E}$ , connecting vertices  $v_1$  to  $v_2$ ,

$$\frac{d}{dt} \int_e |q|^2 dx = -2\Im \int_e (\bar{q}q_x)_x dx = -2(\bar{q}q_x) \Big|_{x=v_1}^{x=v_2}$$

Adding over all the edges, we see

$$\frac{d}{dt} \int_{\mathcal{N}} |q|^2 dx = \sum_{e \in \mathcal{E}} \frac{d}{dt} \int_e |q^{(e)}|^2 dx = -2 \sum_{v \in \mathcal{V}} \bar{q}^{(e)}(v) \sum_{e, v \in e} q_x^{(e)}(v) = 0.$$

A similar computation shows that  $I_1$  is also conserved in time. Following techniques and estimates similar to those presented in [8] we obtain that the network NLS problem is globally well-posed. More precisely, the following result is obtained in [11]:

**Global well-posedness of NLS on  $\mathcal{N}$ .** Given  $q_0 \in H^2(\mathcal{N})$  satisfying the standard junction conditions described above, the NLS system (19) has a unique classical solution  $u \in C^1([0, \infty), L^2(\mathcal{N})) \cap C([0, \infty), H^2(\mathcal{N}))$ .

While the proof of this result is omitted here due to space limitations, it is worth mentioning its implication on the construction presented in Section 3.2 above. Indeed, the global existence in time for the solution  $q(x, t)$ , and in particular of the Dirichlet and Neumann data  $g_0(t)$  and  $g_1(t)$ , implies that the system of equations (16), given these data, is solvable for all times  $t > 0$ , which avoids the delicate issues related to the global solvability of system of the nonlinear, nonlocal hyperbolic equations (16)–(18).

## 4 Numerical experiments

In this final section we present numerical results for the NLS equation posed on simple networks. Among the numerous schemes used for discretizing the NLS equation, we have chosen the celebrated Ablowitz-Ladik (AL) semi-discretization in space

$$iq_j + \frac{1}{2h^2} (q_{j+1} - 2q_j + q_{j-1}) + |q_j|^2 (q_{j+1} + q_{j-1}) = 0$$

where  $h$  is the spatial mesh size of the uniform grid  $\{x_j\}_{j=1}^N$  and  $q_j = q(x_j)$ ,  $j = 1, \dots, N$ . The AL scheme is known to be integrable, in the sense of the inverse scattering theory. Time discretization was done via the 4th order Runge-Kutta method. An alternative approach is to use the Crank-Nicolson discretization in time first, in particular the Besse relaxation scheme introduced in [3], but we will not pursue this here, since from our experiments it appears the same type of scattering is observed.

An initial NLS soliton is set up in the first (leftmost) segment and given an initial velocity to the right towards the interface and second segment. The interface conditions are given by:

$$q^- = q^+ \quad \text{and} \quad q_x^- = \gamma q_x^+.$$

The derivative at the interface  $q_N$  is approximated on the left side by the values at  $k + 1$  points to the left (for the range of speeds and amplitudes simulated we considered  $k = 5$ ):  $q'_{N-} = \sum_{j=0}^k \alpha_j q_{N-j}$  and similarly on the right side  $q'_{N+} = -\sum_{j=0}^k \alpha_j q_{N+j}$ , where  $\alpha_j$  are numerical weights computed as in [17]. Setting the left and right derivatives equal to each other and solving for  $q_N$  yields:

$$q_N = -\frac{1}{(1 + \gamma)\alpha_0} [\alpha_1(\gamma q_{N+1} + q_{N-1}) + \alpha_2(\gamma q_{N+2} + q_{N-2}) + \alpha_3(\gamma q_{N+3} + q_{N-3}) + \dots]$$

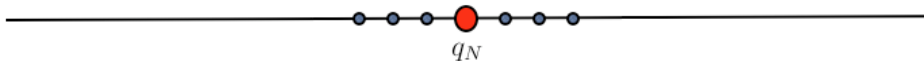


Figure 2: The finite difference scheme uses an uniform grid at both sides of the interface.

Updating the value of  $q_N$  with the value from the above calculation after each iteration in time assures that the continuity conditions at the interface are satisfied. Two different time snapshots are provided in Figure 3 below (before and after the interaction with the interface, located in the middle of the x axis.)

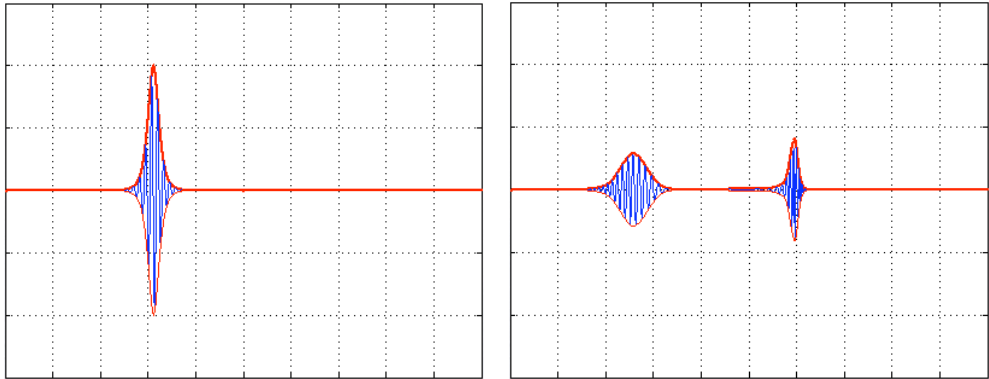


Figure 3: Scattering of pulses off the interface: Pulse moving right before interaction (left figure) and transmitted and reflected pulses after interaction (right figure)

In the first set of numerical experiments, pulses of the same amplitude  $a = 2$  but varying speeds  $c \in [5, 12]$  were launched from the left of the interface (recall that for the NLS solutions speed and amplitude are two independent parameters). We observe that the transmitted and reflected speeds computed indicate a linear relationship with the incident speed. The slight departure from an exact linear relationship is attributed to the way the speeds of the reflected waves are estimated, based on locating the peak of the transmitted and reflected waves and the fact that a uniform grid is used.

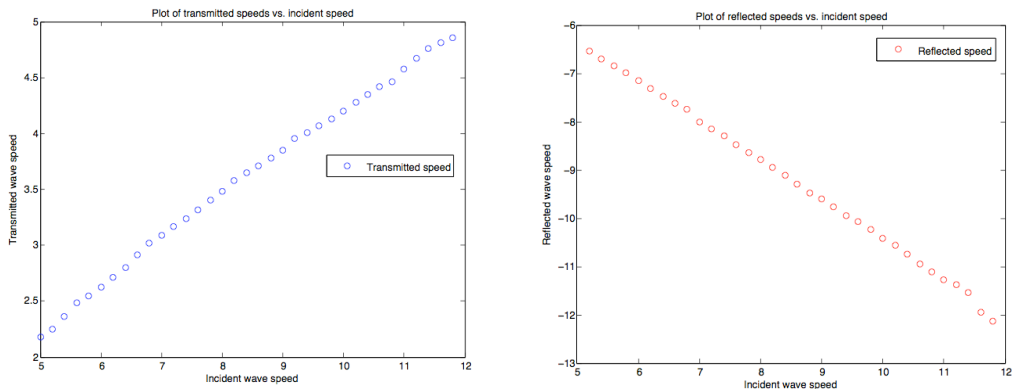


Figure 4. Linear dependence of the speed of transmitted (left) and reflected (right) pulses to the incoming speed. Amplitude of incoming pulse is kept constant ( $a = 2$ ).

Subsequently, the amplitude of the incoming pulse was also varied. Results for various values of initial amplitudes and speeds are displayed in the following figures, the lines representing still the computed speeds for a given amplitude

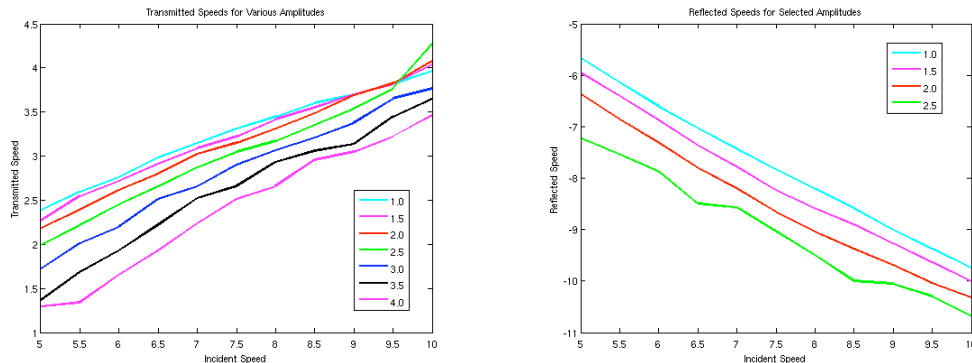


Figure 5. Same as in Figure 4, but results from different amplitudes  $a \in [1, 4]$  are being displayed.

The junction is set up in a similar fashion to the interface problem. Rather than two segments, however, there are three. An initial soliton is again set up in the first (leftmost) segment with an initial rightward velocity. At the interface, the continuity conditions are  $q^{(1)} = q^{(2)} = q^{(3)}$  and  $q_x^{(1)} = q_x^{(2)} + q_x^{(3)}$  where  $q^n$  are the values at each each segment just outside the junction. This time, however, each segment is calculated independently, following the same  $k^{th}$  order approximation for the derivatives at the junction and solving for the updated junction value. After each time iteration the value at the junction for all three segments is updated. The results are similar for the interface problem, with the only change being noticed when the junction is asymmetric.

The code developed for the Y-junction problem above can be easily adapted to simulate the NLS on finite number of edges in a network. Using the same procedures for calculating the junction values, we obtain the following response function at a generic site in the network.

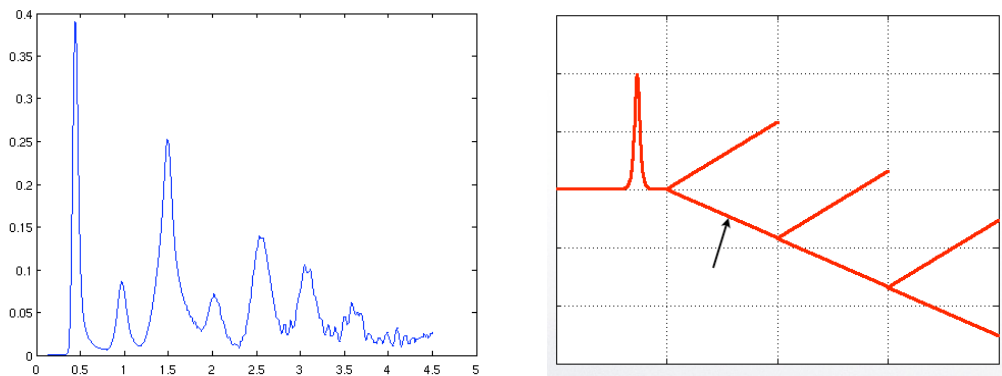


Figure 6: Temporal tracing of  $|q(\cdot, t)|$  (left) at a generic site (marked by arrow) in a 7-edge tree (right)

We conclude with a remark on the discretization that can be done via the developments presented in Section 2 and 3. The discretization of the fractional order operator is done as

follows ([18], [20])

$$g_1^n = g_0^n M_{2,n}^n - e^{-\frac{i\pi}{4}} \frac{2}{\sqrt{2\Delta t}} \sum_{j=0}^n \omega_j M_{1,n-j}^n, \quad \text{where } \omega_j = \begin{cases} \frac{(2k)!}{2^{2k}(k!)^2}, & j = 2k, \\ -\omega_{j-1}, & j = 2k + 1 \end{cases}$$

The system of equations (16) is discretized using the Crank-Nicolson scheme on the lines with slope 1 and -1 in the region  $\Lambda = \{(t, s) | 0 \leq t \leq T, -t \leq s \leq t\}$ . While the resolution of the continuous time system is currently out of reach, the numerical implementation of these schemes can be done with relative ease and will be reported elsewhere.

## 5 Conclusions

The study of initial-boundary value problems for nonlinear dispersive equations such as the NLS posed on simple networks provides further insight into the nature of the scattering of nonlinear pulses off junctions. The linear relationship between the transmitted and reflected wave speeds to the incoming wave speed is a phenomenon that has been observed numerically in this and other related studies. In the NLS context, because of the amplitudes and speeds of incoming pulses can be chosen independent of each other, the phenomenology is much more complex than that encountered in other equations. Further investigations are underway as to whether the analytic approach involving the Dirichlet-to-Neumann map presented in this study may lead to a theoretical interpretation of this linear scattering behavior, as the fully numerical scattering experiments indicated above. In addition, more sophisticated numerical schemes, such as the pseudo-spectral collocation method, and their stability and convergence analyses, are being developed to better capture the dynamics of pulses near the bifurcations.

## References

- [1] J. Alastruey, K.H. Parker, J. Peiro, S.J. Sherwin: Analyzing the pattern of pulse waves in arterial networks: a time-domain study, *J. Eng. Math.*, **64** N. 4 (2009), 331–351.
- [2] X. Antoine, A. Arnold, C. Besse, M. Ehrhardt and A. Schdle: A review of transparent and artificial boundary conditions techniques for linear and nonlinear Schrödinger equations, *Commun. Comput. Phys.* **4**, No. 4 (2008), 729–796.
- [3] C. Besse: A relaxation scheme for the nonlinear Schrödinger equation, *SIAM J. Numer. Anal.* **42**, No. 3, (2004), 934–952.
- [4] G. Biondini, G. Hwang: Solitons, boundary value problems and a nonlinear method of images, *J. Phys. A: Math. Theor.* **42** (2009), 205207.
- [5] J. L. Bona, R. C. Cascaval: Nonlinear dispersive waves on trees, in *Canadian Applied Mathematics Quarterly*, **16**, No. 1 (2008), 1–18.

- [6] J. L. Bona, A. S. Fokas: Initial-boundary-value problems for linear and integrable nonlinear dispersive partial differential equations, in *Nonlinearity*, **21** (2008), T195–T203.
- [7] A. Boutet de Monvel, A.S. Fokas, D. Shepelsky: Analysis of the global relation for the nonlinear Schrödinger equation on the half-line, *Lett. Math. Phys.* **65** (2003), 199–212.
- [8] R. Carroll, Q. Bu: Solution of the forced nonlinear Schrödinger (NLS) equation using PDE techniques, *Applicable Analysis*, **41**, (1991), 33–51.
- [9] R. C. Cascaval, F. Gesztesy, H. Holden, Y. Latushkin: Spectral analysis of Darboux transformations for the focusing NLS hierarchy, *Journal D'Analyse Mathématique*, **93** (2004), 139–197.
- [10] R. C. Cascaval: A Boussinesq model for pressure and flow velocity waves in arterial segments, preprint.
- [11] R.C. Cascaval: Nonlinear Schrödinger equation posed on a network, in preparation, 2010.
- [12] A. S. Fokas: Boundary-value problems for linear PDEs with variable coefficients, *Proc. R. Soc. Lond. A* **460** (2004), 1131–1151.
- [13] A. S. Fokas. *A Unified Approach to Boundary Value Problems*, CBMS-NSF Regional Conference Series in Applied Mathematics, SIAM 2008.
- [14] M. Garavello, B. Piccoli: *Traffic Flow on Networks*, AIMS 2006.
- [15] N. Golding, W. L. Kath and N. Spruston: Dichotomy of action potential backpropagation in CA1 pyramidal neuron dendrites, *J. Neurophysiology*, **86** (2001), 2998–3010.
- [16] Y. Latushkin, V. Pivovarchik: Scattering in a forked-shaped waveguide, *Integr. Eq. Oper. Theory* **61** (2008), 365–399.
- [17] R. LeVeque: *Finite Difference Methods for Ordinary and Partial Differential Equations*, SIAM 2007.
- [18] I. Podlubny: *Fractional Differential Equations*, Academic Press 1999.
- [19] Z.A. Sobirov, D.U. Matrasulov, K.K. Sabirov, S.Sawada, N. Nakamura: Soliton solutions of nonlinear Schrödinger equation on simple networks, preprint, arXiv: 0912.1687v1.
- [20] C. Zheng: Exact nonreflecting boundary conditions for on-dimensional cubic nonlinear Schrödinger equations, *J. Comp. Physics*, **215** (2006), 552–565.
- [21] A. Zisowsky, M Ehrhardt: Discrete artificial boundary conditions for nonlinear Schrödinger equation, *Mathematical and Computer Modeling*, **47** (2008), 1264–1283.